International Journal of Scientific Research and Modern Education (IJSRME)
ISSN (Online): 2455 – 5630
(www.rdmodernresearch.com) Volume I, Issue I, 2016

STUDY ON SECOND ORDER NONLINEAR PROPERTIES OF ORGANIC MATERIAL: GUANIDINE HYDROGEN MALEATE SINGLE CRYSTALS

D. Sathya*, V. Sivashankar*, S. Anbarasu & D. Prem Anand***
* Department of Physics, St. Xavier's College, Palayamkottai, Tamilnadu
** Loyola College, Mettala, Nammakkal, Tamilnadu

Abstract:

For the investigation of Non linear properties in particular second harmonic generation (SHG) of the organic crystals Guanidine hydrogen Maleate are synthesized. As grown (GuMlt) single crystals subjected into X- ray diffraction studies it represents the title compound have orthorhombic structure and non centrosymmetric space group, Pca21. The functional groups of the title compound observed using FTIR and FTRAMAN spectra. The powder second harmonic generation measurement of (GuMlt) single crystals showed that its nonlinear efficiency is 1.2 times larger than that of KDP. Optical transparency of the (GuMlt) single crystals measured by UV- Vis spectrum shows the cutoff frequency at 298 nm. The thermal behavior is studied by TG/TDA analysis shows that the (GuMlt) single crystals have melting point near 200^{0}C. Optical characterization, mechanical and Dielectric behavior of the (GuMlt) single crystals are reported for the first time which establishes the usefulness of the crystal for various up to electronic applications.

Key Words: Optical Materials, Crystal Growth, Thermo Gravimetric Analysis & Dielectric Properties

1. Introduction:

Focusing the applications in the fields like optoelectronics, photonics and optical devices, makes interest in the investigation of new nonlinear optical materials. Variety of organic and inorganic NLO crystals is grown in this trend. But, research in organic NLO single crystals is more advantageous when compared to inorganic nonlinear materials. Despite, in organic materials the ions are easily incorporated into the lattice and also the bond strength, optical susceptibility dielectric constant, molecular interactions are attracting the attention rapidly [1- 16]. From this view, the search of nonlinear properties in organic crystals particularly having second harmonic generation (SHG) the Guanidinium hydrogen male ate single crystals is synthesized. Guanidinium crystals exhibit numerous applications in the optoelectronic field. Because of the strong basic character of Guanidine, it can be considered super bases used in protonation to generate resonance stabilized Guanidinium cations [17-30]. Maleic acid is the simple carboxylic acid having carbon- carbon double bond which is applicable in nonlinear optics. Maleic acid acts with other organic molecules as an acidic ligand to form salts through specific electrostatic or hydrogen bond interactions. Guanidine cations are anhydrous when it reacts with carboxylic acid and also acts as a very good oxidizing agent, it exhibits light emission phenomena. Guanidine cation gives hydrogen bonding interactions with carboxylate and to a lesser extent, O acceptors of the anion to the formation of GuMlt single crystals. H-bonds used to form the non- centro symmetric structures which lead to the NLO properties [18, 30-37]. The crystal structure of Guanidine hydrogen Male ate consists of planar confirmation. ie, strong hydrogen bonds between the guanidinium cations & carboxylic anions which make the orthogonal arrangement with one carboxylic group present in the Maleic (cisbutenedioic) acid [18]. To the best of our knowledge there is no report on the GuMlt crystals for NLO

application by Kurtz- Perry Powder SHG method, elemental, Uv-Vis study, hardness measurement and TG/DTA studies and the dielectric properties.

2. Experimental Procedure:

Single crystals of Guanidine hydrogen maleate (GuMlt) are grown by slow evaporation method. The maleic acid [C3H3O2COOH, 99.9%] and guanidinium carbonate[C(NH2)3CO3, 99%] taken in the equimolar ratio and dissolved in double distilled water. The solution is stirred continuously using magnetic stirrer for 5 hours. The reactor is filtered, kept undisturbed in room temperature for slow evaporation. The acidic portion of maleic acid is the carboxyl group; it reacts with the Guanidine cation to form GuMlt single crystals. The final product of synthesis is purified by repeated crystallizations from water solution. The colorless, transparent crystals are of size 15 x 10 x 8 mm 3 obtained after 20 days of the growth as shown in Fig. 1.

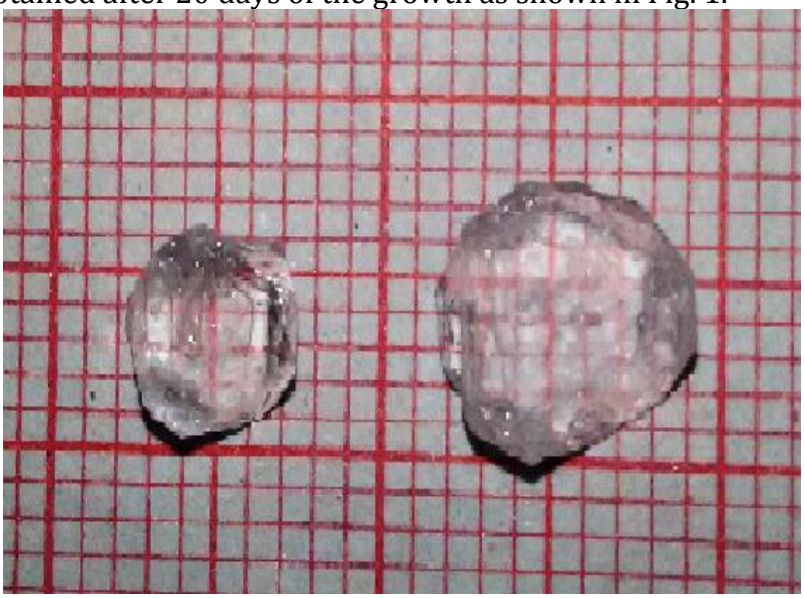

Figure 1: As Grown Gumlt Single Crystals

3. Results and Discussion:

3.1 CHN Analysis:

The result of the CHN analysis is presented in Table 1. Analysis of Carbon, Hydrogen, Sulfur and Nitrogen is carried out using Vario EL III Elementar. Theoretical values of CHNS are found by the molecular formula Guanidine hydrogen Maleate [CH6N3 + C4H304 -]. The experimental and calculated values of C, H, N and S agree with each other which confirm the formation of GuMlt crystal.

Element	Experimental Values (%)	Theoretical Values (%)
C	21	19.26
H	7.84	7.62
N	33.26	32.83
S	0.08`	0.08

Table 1: CHNS Analysis data for GuMlt single crystals

3.2 XRD Measurements:

Single Crystal XRD study has been carried out to confirm the crystallinity and to calculate lattice parameters of the grown crystal. X- ray diffraction data are collected using an ENRAF NONNIUS- CAD 4 single crystal X- ray diffract meter with MoKα (λ= 0.71073 Å) radiation at room temperature. GuMlt single crystals belongs to the orthorhombic system, space group Pca21 with lattice parameters a=19.197 A^0, b= 3.679 A^0, c= 11.324 A^0,V= 812 A^3 .These values are in well agreement with the reported values

of L. Golic et al [38] confirms the identity of the grown single crystals. A powder XRD pattern of the grown GuMlt single crystals is recorded using BRUKER D8 ADVANCE powder diffract meter with Cu Ka radiation (λ= 1.5418A ˚). The sample is scanned at a rate of 10˚ per minute in the 2θ range of 10–700. All the observed reflection lines in XRD pattern are indexed using the Treor program. Powder XRD analysis is also taken for GuMlt single crystals. d spacing with respect to the hkl values are depicted in Table 2 and the Fig. 2 shows the peak intensity of GuMlt single crystals.

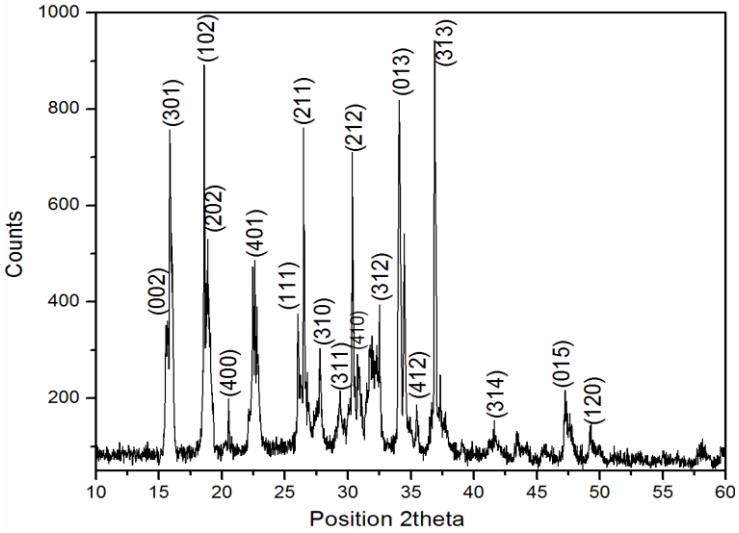

Figure 2: PXRD analysis for GuMlt single crystals

d[Å]	h	k	l
5.69727	0	0	2
5.5827	3	0	1
4.77074	1	0	2
4.69517	2	0	2
4.32176	4	0	0
3.95838	4	0	1
2.81309	5	0	1
3.42225	2	1	0
3.36513	2	1	1
3.20752	3	0	3
3.04309	3	1	1
2.94517	2	1	2
2.89569	4	1	0
2.76225	3	1	2
2.63014	0	1	3
2.60214	4	1	2
2.43614	3	1	3
2.16967	3	1	4
1.92319	0	1	5
1.83832	1	2	0
1.54063	1	2	4

Table 2: PXRD data for GuMlt single crystals

3.3 Second Harmonic Generation Study:

The study of NLO conversion efficiency has studied using the Kurtz- Perry powder technique. A Q- switched Nd: YAG laser beam of wavelength 1064nm with an

input power of 300 mJ/pulse width of 10ns with a repetition rate of 10Hz is used. The fine powder of GuMlt single crystals is taken into the tightly packed micro capillary tube. It is mounted on the path of the laser beam radiation of energy 9.6 mJ. The output of the sample is monochromotated at the intensity of 532nm emits green light. The emission of the Green light confirmed the presence of non linear optical property. Potassium dihydrogen phosphate (KDP) also powdered into the identical size is used as reference material in this experiment. SHG value of the title compound is found to be 1.2 times greater than that of KDP.

3.4 UV Visible Spectral Study:

The UV spectrometer results are taken in the region 200 to 1200 nm using Shimadzu 2410 UV spectrophotometer. The transmittance spectrum of GuMlt single crystal is shown in Fig.3. The lower cutoff wavelength of the GuMlt single crystals is found to be 298nm. There is a group strong absorption between the wavelengths of 200 to 298nm after that no absorption till 1200nm. The wide optical window is seen in the crystal and plays a vital role NLO application. Which leads to study the NLO property and it confirms to be useful in optoelectronic applications. Band gap energy of GuMlt single crystals measured from the graph Energy (hν) Vs (αhν) ½ as shown in Fig.4. By extrapolating the linear portion of the curve to zero absorption the indirect band gap energy is found to be 4.4 eV. Here α- absorption coefficient, hν- photon energy. Band gap value is comparable to that the guanidine compounds [39].

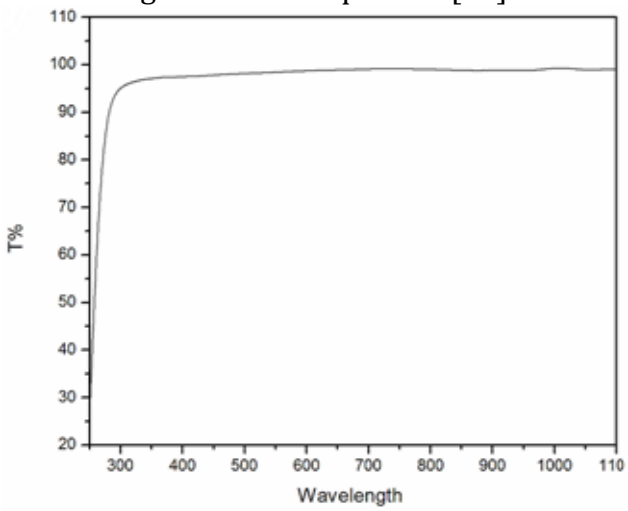

Figure 3: Transmittance spectrum of GuMlt single crystals

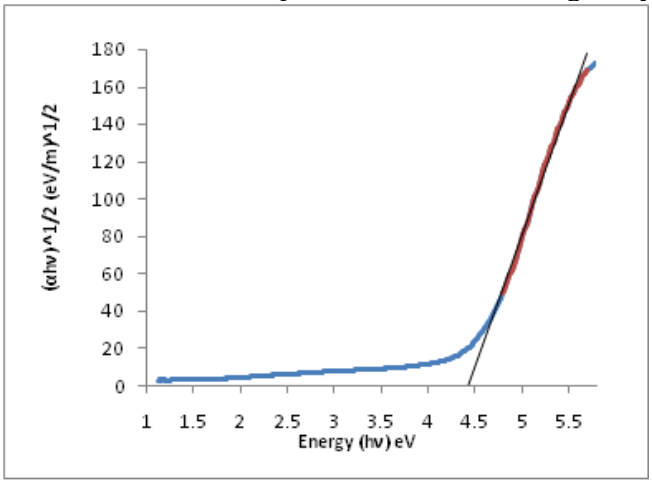

Figure 4: Energy (hν) Vs (αhν) 1/2 graph of GuMlt single crystals

3.5 Vibrational Studies:

Fourier transform infrared spectrometry spectrum is recorded in Bruker IFS-66V spectrometer in the range 4000 to 400 cm-1. FTIR and FT Raman spectrum of GuMlt single crystals are shown in Fig.5. For infrared region the following vibrations observed. OH- Streching vibration is observed at 2501 cm-1. The bands are observed at 1672 cm-1 is due to the presence of C=C stretching, 1390 cm-1 confirms carboxylate group. C-H bending and carboxylate group deformation are observed at 856 cm-1 and 623 cm-1 respectively. C=O carbonyl group deformation is observed at 535 cm-1. C-N stretching vibration is observed at 1216 cm-1. The bands in the range 3400-3100 cm-1 shows symmetric and asymmetric stretching of N-H bonds [40]. The Raman spectra are measured using Bruker RFS spectrophotometer 50 -5000 cm-1. C- H stretching is observed in the region 3043 cm-1 , 2370 cm-1 and 1673 cm-1 shows the O- H stretching and C= C stretching vibrations. 1393 cm-1 observes the symmetric deformation of carboxylate group COO-. CO2 stretching and wagging observed at 643 cm-1 and 544 cm-1 respectively [40]. The above interpretation in Raman spectra are indicates the functional groups of the GuMlt single crystals.

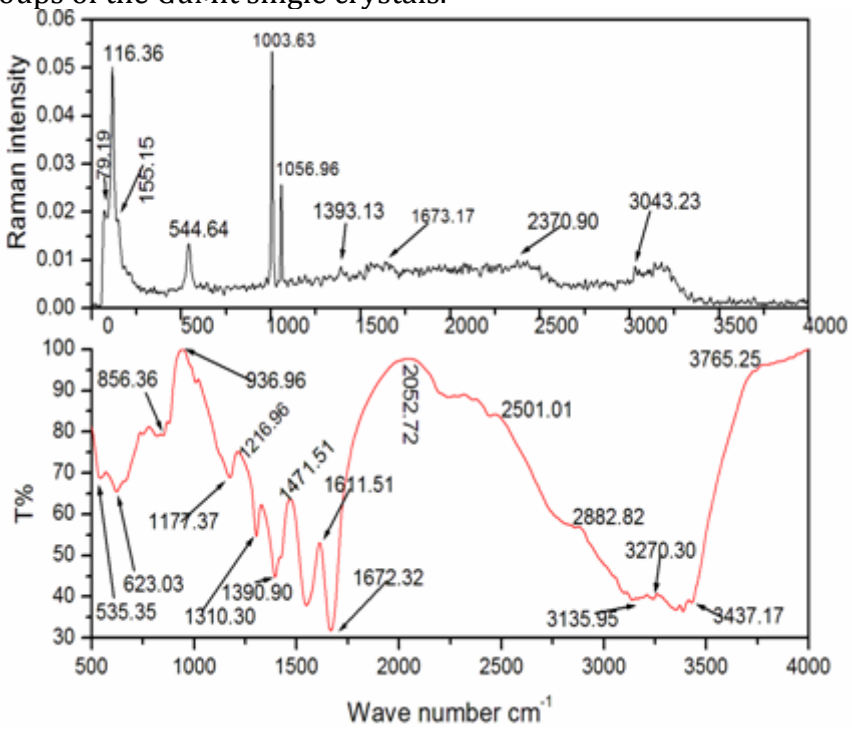

Figure 5: FTIR and FT Raman spectrum of GuMlt Single crystals

3.6 Thermal Analysis:

The TG/DTA trace of GuMlt single crystals is shown in Fig.6. Thermo gravimetric and differential thermal analysis gives information regarding phase transition, presence of water molecules and different stages of decomposition of the crystal system. The thermo grams (TG and DTA) are carried out in a dynamic air atmosphere from 30^{0}C to 800^{0}C using STA 1500 thermal analyzer. In TG curve a small variation in mass observed between 170^{0}C - 200^{0}C, which is due to the acid-catalyzed dehydration which is the melting point of the Guanidine hydrogen Male ate single crystal. There is a sudden decrease in mass (approximately 70%) at 254^{0}C it continues up to 315^{0}C due to the decomposition of C-H and C-O bonds. Good crystalline nature confirmed by the sharp decrease in peak. Nearly 400^{0}C simple endothermic peaks observed which corresponds to the remaining guanidine compounds. After 700^{0}C, there is no mass loss and the GuMlt single crystals are fully decomposed [41]. In DTA, simple endothermic arises at 170^{0}C is

due to dehydration which is the melting point of the title compound. In DTA, large endothermic peaks are located between 215- 292^{0}C which corresponds to the oxidation of flammable volatile compounds [42]. At 400^{0}C exothermic peak is observed which corresponds to the oxidation of aromatic components. A small endothermic peak observed at 414^{0}C shows that evaporation of volatile products. Exothermic peak at high temperature (636^{0}C) is due to the evaporation of carbonaceous compounds [41].

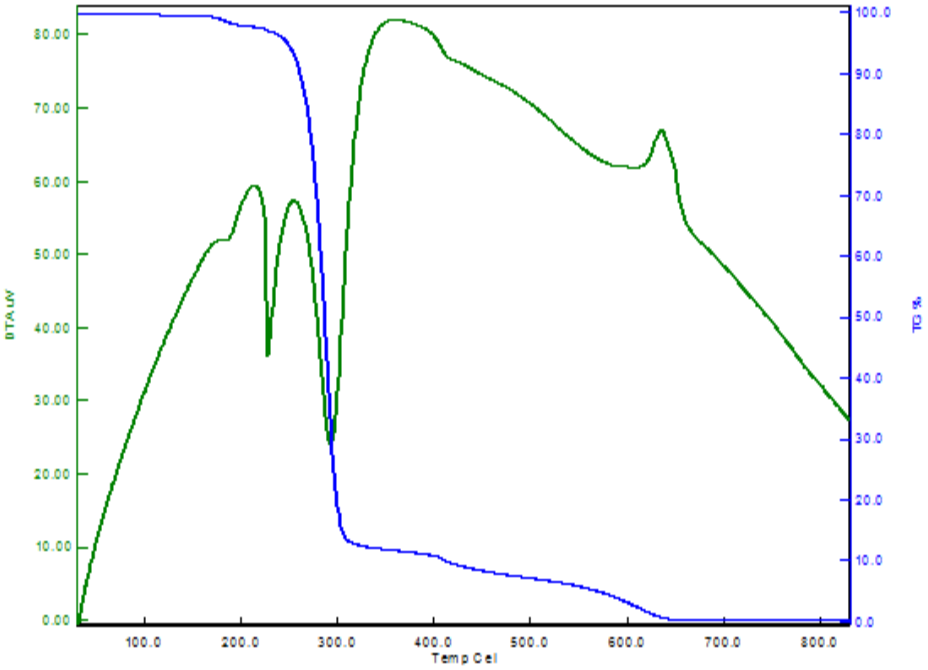

Figure 6: TG- DTA Graph of GuMlt Single crystals

3.7 Micro Hardness Analysis:

The mechanical property of the GuMlt single crystal is studied by micro hardness tester. Hardness of the material is a measure of resistance that offers to deformation. Micro hardness test is observed using HMV SHIMADZU micro hardness tester with diamond indentor. Figure 7 Shows that the Load in kg Vs Hv in kg/mm^3 .The well polished crystals are mounted on the platform of the tester and the loads of different magnitudes are applied for a particular time interval of every 15s.

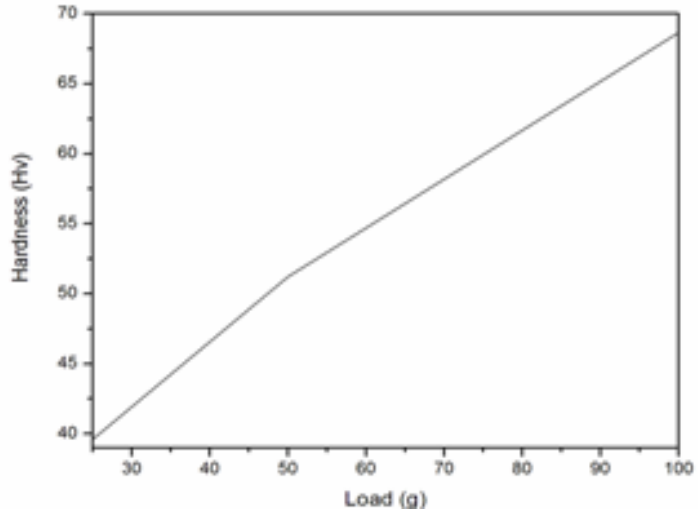

Figure 7: Load (g) Vs Hardness graph (Hv) of GuMlt Single crystals

Micro hardness of the solid materials depends on the applied load for indentation. This is known as indentation size effect (ISE). The hardness Hv increased

gradually with the increase of load which shows the reverse ISE [43]. The micro hardness value (Hv) was calculated using the formula, Hv = 1.8544(P/d2) kg/mm2 Where, P- load, d- average diagonal length. The load applied till 100gm after this crack was developed due to the formation of internal stress. The work hardening coefficient n is calculated using Meyer's law, P = k1dn, Where, k1 is a material constant, n is the Meyer index. Figure 8 shows the Meyer index slope of Log d Vs Log P. The value of n is found to be 3.154. The concept of Kick is, the exponent is n >2 for reverse ISE and n=2 is independent of the applied test load. According to Onitsch, if n is above 1.6 the material is under soft category. For the values below 1.6 the materials belongs to the hard category [44, 45]. From this conclusion, we observed that GuMlt having the soft material nature. So the title compound having the soft material nature and this will be useful for the telecommunication application and in solar cells.

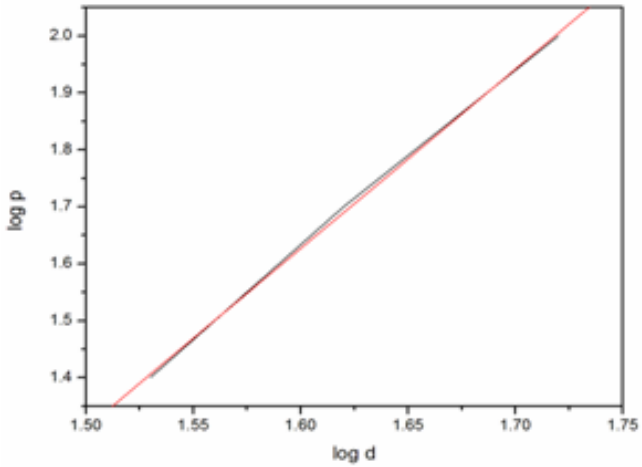

Figure 8: Log P Vs Log d Graph of GuMlt single crystals

3.8 Dielectric Studies:

Dielectric studies of GuMlt single crystal is carried out at various frequencies and temperatures. This Dielectric measurement gives information about the polarization nature of the materials. It is performed on a Guanidinium Maleate single crystal using a HIOKI HITESTER model 3532- 50 LCR meter. The sample is placed inside a dielectric cell whose capacitance is measured at various temperatures 60, 80, 100,120 and 150^{0}C respectively for different frequencies. A sample of crystal having silver coating on the electrodes so that it behave as a parallel plate capacitor. Dielectric constant of GuMlt single a crystal for various temperatures is shown in fig.9.

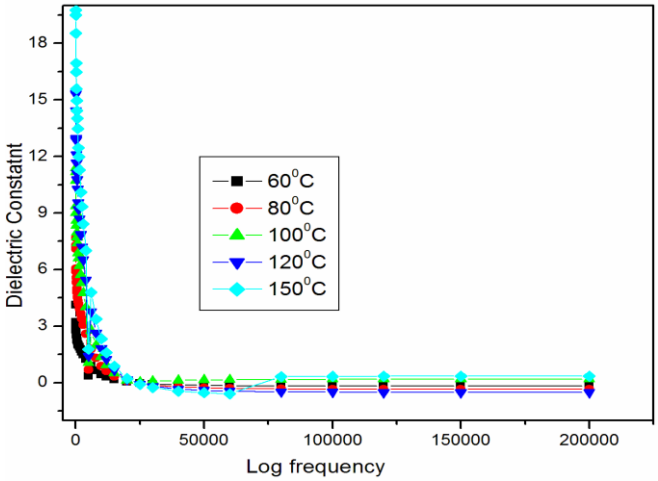

Figure 9: Dielectric constant Vs Log frequency graph of GuMlt single crystals

It is evidence from the graph that dielectric constant of GuMlt single crystal increases with increase in temperature. Dielectric constant of GuMlt single crystal decreases with increase in frequency and attain saturation at higher frequency for various temperature from 60 to 150^{0}C. The dielectric constant has High value at low frequency is due to the space charge polarization [46-48]. According to Miller's rule [49] low dielectric constant at high frequency is the essential property for SHG applications. GuMlt crystal is potential candidate for opto electronic applications. Dielectric loss Vs frequency of GuMlt crystal for various temperatures is shown in fig.10. Dielectric loss is low at high frequencies. It is observed that the dielectric loss is 0.41 at the maximum frequency of 2 MHZ. Low value of dielectric loss at higher frequencies is suitable for opto electronic applications. This lower value of dielectric constant shows the crystal is free from defects [50].

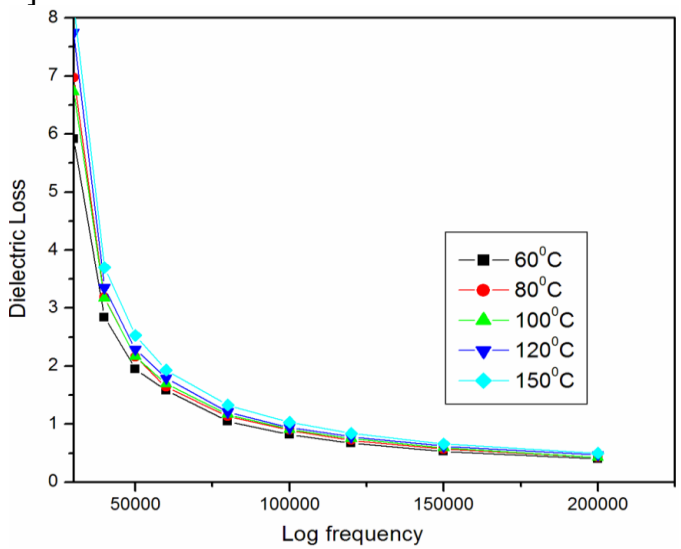

Figure 10: Dielectric loss Vs log Frequency graph for GuMlt single crystals

4. Conclusion:

Good quality of organic material for opto - electronic application is synthesized, and single crystal GuMlt has been grown by slow evaporation technique for optical applications. Single crystal XRD has been carried out to find the cell parameters of the crystal. The crystalline nature of the grown crystal is analyzed by powder XRD. Various functional groups present in the crystal are confirmed by FTIR, FTRAMAN spectrum. The result of the SHG test conducted on the experimental crystal confirms the non-linear nature of the crystal. UV- Visible spectral studies show that GuMlt single crystals have the cutoff wavelength around 298 nm and this gives the indirect band gap of 4.4 eV. The crystal is transparent in the entire visible region which makes the crystal has the potential application in optical communication. From TG/DTA analysis melting and decomposition temperature and the purity of the title compound was found and the crystal is thermally stable upto 170^{0}C. Mechanical studies using Vicker's micro hardness test reveals that GuMlt single crystal belongs to the reverse ISE and crack developed for load above 100 g. From the studies, hardening coefficient is found to be 3.154. The observed low Dielectric constant and dielectric loss suggest that the material suitability for NLO applications.

5. Acknowledgment:

The authors are grateful to Department of Science and Technology, Government of India for the financial assistance [SERB/F/3557/2012-13 Dated: 26-09.2012]. The authors acknowledge Saif - IIT Madras for XRD and FT- Raman analysis.

6. References:

1. Duorong Yuan, Zhenwu Zhong, Mingguo Liu, Dong Xu, Qi Fang, Yonghong Bing, Suoying Sun, Minhua Jiang, J. Crystal Growth 1998; 186: 240.
2. R. Ittyachan, P. Sagayaraj, Journal of Crystal Growth 2003; 249: 557–560.
3. Tanusri Pal, Tanusree Kar, Gabriele Bocelli, and Lara Rigi, Cryst. Growth Des. 2003; 3(13)1.
4. S. A. Martin Britto Dhas and S. Natarajan, Cryst. Res. Technol. 2007; 42 (5): 471 – 476.
5. S. Devashankar, L. Mariappan, P. Suresh kumar, M. Rathnakumari, J. Crystal Growth 2009; 311: 4207–4212.
6. Hansen shou, jianping ye, Qun yu, Journal of Luminescence 1988; 42: 29-34.
7. G. Bator, Th. Zeegerrs – Huyskens, R. Jakubas, J. Zaleski, J. Mol. Struct. 2001; 570: 61.
8. Ananthi, S. Mary Delphine, M. Mary Freeda, R. Krishna Priya, Abdul Wahab Almusallam, Recent Research in Science and Technology, 2011; 3(1): 32.
9. P.Selvarajan, J.Glorium Arul Raj, S.Perumal, Journal of Crystal Growth 2009; 311: 3835–3840.
10. B. Narayana Moolya, S.M. Dharmaprakash, Journal of Crystal Growth 2006; 290: 498– 503.
11. Arijit Mukherjee, Karuna Dixit, Siddharth, P. Sarmab, Gautam R. Desiraju, IUCrJ 2014; 1:228-239.
12. Ge´raldine Lenoble, Pascal G. Lacroix, Jean Claude Daran, Inorg. Chem. 1998; 37: 2158-2165.
13. Graham Smith, Daniel E.Lynch, Karl A. Byriel, Colin H. L. Kennard, J. Chemical Crystallography 1997; 27(5): 307-317.
14. Kin-Shan Huang, Doyle Britton, Margaret C. Ettera, Stephen R. Byrn, J. Mater. Chem. 1997; 7(5):713–720.
15. Yukiko Kusano, Keiji Ohno, Takashi Fujihara, Acta Cryst. 2015; E71:0623-0624.
16. Ignez Caracelli, Julio Zukerman-Schpector, He´lio A.Stefani, Bakhat Ali, Edward R. T. Tiekink, Acta Cryst. 2015; E71: 0582-0583.
17. P. Koteeswari, S. Suresh, P. Mani, American Journal of Condensed Matter Physics 2012; 2(5): 116-119.
18. Ermelinda M. S. Mac, Rui Fausto, Jan Lundell, Mika Peterson, Leonid Khriachtchev, Markku Rasanen, J. Phys. Chem. A 2001; 105 (15): 3922.
19. U. Karunanithi, S. Arulmozhi, M. Dinesh Raja, J. Madhavan, International Journal of Engineering Research and Development, 2012; 3 (11): 51.
20. Sergey G. Arkhipov, Boris A. Zakharov, Elena V.Boldyreva, Acta Cryst. 2013; C69: 517–521.
21. R. Vijayraghavan, Usman Ali Rana, Gloria D. Elliott, Douglas R. MacFarlane, Energy Technol, 2013; 1: 609-612.
22. G. Bator, Th. Zeegers- Huyskens, R. Jakubas, J. Zaleski, J. Mol. Struct 2001; 570:61.
23. Michaela Fridrichova, Ivan Nemec, Ivana Cisarova, Petr Nemec, CrystEng.Comm. 2010; 12: 2054.
24. Graham Smith, Urs D. Wermuth, Jonathan M. White, Acta Cryst. 2007; E63: 0867-0868.
25. M. Drozd, D. Dudzic, Spectrochimica Acta Part 2012; A 89: 243– 251.
26. Grottel, A. Kozak, A.E. Kozioi and Z. Pajak, J. Phys.: Condens. Matter 1989; 1: 7069- 7083.
27. Z. Pajak, and J. Zaleski, Solid State Communication. 1994; 91: 821.

28. M. Grottel, A. Kozak, and Z. Pająk, Z. Naturforsch. 1995; 50A: 742-748.
29. A. Kozak, M. Grottel and Z. Pająk, Acta physica polonica A 1993; 83.
30. M. Drozd, Materials Science and Engineering B 2007; 136: 20–28.
31. Graham Smith, Urs D. Wermuth, David J. Young and Jonathan M. White Acta Cryst. 2006; E62: o3912–o3914.
32. Matthew T. Allingham, Andrew Howard-Jones, Patrick J. Murphy, Dafydd A. Thomas and Peter W. R. Caulkett, Tetrahedron Letters 2003; 44: 8677–8680.
33. M. Drozd, Spectrochimica Acta Part A 2006; 65: 1069–1086.
34. Michel Fleck, Ladislav Bohatý , Ekkehart Tillmanns, Solid State Sciences 2004; 6: 469– 477.
35. William T. A. Harrison, and Mark L. F. Phillips, Chem. Mater., 1997; 9 (8): 1837-1846.
36. Ken Sakai, Norinobu Akiyama,Mina Mizota, Kazuo Yokokawa and Yoshimi Yokoyama, Acta Cryst. 2003; E59: 408-410.
37. C. Alosious Gonsago, Helen Merina Albert, S. Janarthanan, A. Joseph Arul Pragasam, International Journal of Applied Physics and Mathematics, 2012; 2 (6) : 422.
38. L. Golic, I. Leban, and S. Detoni, Journal of Crystallographic and Spectroscopic Research, 1985; 15(3).
39. V. Sivashankar R. Siddheswaranb, P. Murugakoothan, Materials Chemistry and Physics, 2011; 130: 323– 326.
40. George Socrates, Infrared and Raman Characteristic Group Frequencies, Tables and Charts, John Wiley & Sons, Ltd. England: 2001.
41. Ming gao, caiyun sun, kai zhu, Journal of thermal analysis and calorimetry 2004; 75: 221–232.
42. A. M. A. Nada, H. A. Yousef and S. El-Gohary, J. Therm. Anal. Cal. 2002; 68: 265.
43. K. Senthil, S. Kalainathan, F. Hamada, M. Yamada, P.G. Aravindan, Optical Materials, 2015; 46: 565-577.
44. M. Hanneman, Metall. Manch. 1941; 23: 135–140.
45. Onitsch EM. The present status of testing the hardness of the materials. Microscope. 1950; 95:12.
46. P.C. Thomas, S. Aruna, J. Packiam Julius, A. Joesph Arul Pragasam, P. Sagayaraj, Cryst. Res Technology 2006; 41: 1231 -1235.
47. B. Narshimha, R. N. Choudhary, K. V. Roa, Mater. Sci 1988; 23: 1416.
48. Jyoti Dalal, Nidhi Sinha, Binary Kumar, Optical materials 2014; 37: 457-463.
49. U. Von Hundelshausen, Phys. Letters 1971; 34A: 405-406.
50. Christo Balarew, Rumen Duhlev, J. Solid State Chem 1984; 5(1): 1-6.